Effect of Segmentation Uncertainty on the ECGI Inverse Problem Solution and Source Localization

Narimane Gassa[1,2,3], Machteld Boonstra[7], Beata Ondrusova1[6], Jana Svehlikova[6], Dana Brooks[4], Akil Narayan[5], Ali Salman Rababah[8], Peter van Dam[7], Rob MacLeod[5], Jess Tate[5], Nejib Zemzemi[1,2,3]

[1] Electrophysiology and Heart Modeling Institute (IHU-Lyric), Pessac, France
[2] Institute of Mathematics, University of Bordeaux, Talence, France
[3] INRIA Bordeaux Sud-ouest, CARMEN Team, Talence, France
[4] Northeastern University College of Engineering, Boston, USA
[5] University of Utah, Salt Lake City, USA
[6] Institute of Measurement Science, SAS, Bratislava, Slovakia
[7] UMC Utrecht, Utrecht, The Netherlands
[8] Royal Medical Services, Amman, Jordan

Abstract

Electrocardiographic Imaging (ECGI) is a promising tool to non-invasively map the electrical activity of the heart using body surface potentials (BSPs) and the patient specific anatomical data. One of the first steps of ECGI is the segmentation of the heart and torso geometries. In the clinical practice, the segmentation procedure is not fully-automated yet and is in consequence operator-dependent. We expect that the inter-operator variation in cardiac segmentation would influence the ECGI solution. This effect remains however non quantified.

In the present work, we study the effect of segmentation variability on the ECGI estimation of the cardiac activity with 262 shape models generated from fifteen different segmentations. Therefore, we designed two test cases: with and without shape model uncertainty. Moreover, we used four cases for ectopic ventricular excitation and compared the ECGI results in terms of reconstructed activation times and excitation origins.

The preliminary results indicate that a small variation of the activation maps can be observed with a model uncertainty but no significant effect on the source localization is observed.

Introduction

The inverse problem in cardiac electrophysiology, also known as electrocardiographic imaging (ECGI), has been a research topic for decades as it may be a powerful tool for the treatment and diagnosis of cardiac arrhythmia.

ECGI non-invasively estimates electrical activity of the heart using body surface potential measurements obtained are combined with a specific CT/MRI based anatomical models and defined electrode positions. However, the problem is known to be ill-posed; the uncertainty of the mathematical model mainly due to the different hypotheses stated and its parameters generate modeling errors and uncertainty in the inverse solution.

Moreover, ECGI relies on image segmentation for geometry creation. Since the process is operator dependent, it also introduces more uncertainty into the solution as it has shown that the segmentation variability affects estimated ventricular potentials [1]. Despite the previously studies conducted on the statistical shape analysis of ventricular segmentation variability the effect of this variation on ECGI remains unexplored [2, 3].

More sources of uncertainties likely affects the ECGI solutions including the position of the heart within the torso mainly affected by respiration or changes in body position.

Therefore, in this study, we focus on the effect of segmentation variability on ECGI estimations of cardiac activation.

Methods

1. Anatomical Data

Fifteen different cardiac segmentations from the same single subject CT-scans were created by different researchers within the consortium for ECG Imaging (CEI, ecg-imaging.org). Then, these segmentations were analyzed using ShapeWorks to study the variability in segmen-

tation [4]. Therefore, 1024 control points were obtained which were evenly distributed over the surface. From the derived statistical model, 262 cardiac shape models were obtained as previously described in [2].

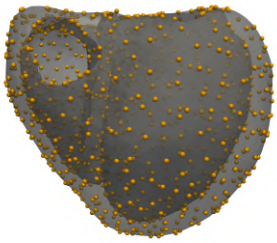

Figure 1. Representative example of one cardiac shape model with the control points.

2. Forward problem

To study solely the effect of segmentation variability on the inverse problem, body surface potentials (BSP) were computed using all 262 cardiac models using one torso model with 120 electrodes [5]. Specifically, the monodomain model was used to simulate the electrical wave propagation. In each of the 262 cardiac model we used four stimulation protocols of ventricular focal excitation : left ventricular (LV), right ventricular (RV), left ventricular septum, and apex as shown in Figure 2. On the torso surface, the electrical potential is computed using the pseudo-ECG approximation and is described by a Laplace equation and satisfies

$$\mathrm{BSP}(x,y,z) = \frac{1}{4\pi}\int_{\Omega_\mathrm{H}} \nabla V_\mathrm{m}.\nabla\left(\frac{1}{r(x,y,z)}\right),$$

where V_m stands for the trans-membrane potential, Ω_H the heart domain and r is the Euclidean distance between the electrode at position (x,y,z) and a point of the heart.

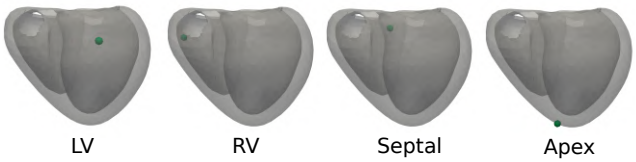

Figure 2. Ventricular stimulation protocols.

3. Inverse problem : MFS

We used the simulated BSP to estimate the cardiac activation sequence using the Method of Fundamental Solutions (MFS). We approach the solution of the elliptic problem given by the Laplace equation by a linear combination of fundamental solutions of the differential operator which is, in our case, the *Laplacian*. These solutions will be located on a set of points called virtual source points $y_j, j = 1 \dots M$ over an auxiliary surface of $\hat{\Omega}_T$ located outside of the domain of interest Ω_T as described in [6].

The potentials are expressed as $u(x) = a_0 + \sum_{i=1}^{M} f(x,y_j)a_j$, where $x \in \Omega_T$, y_j are the virtual source points and $a_j, j = 1 \dots M$ are their corresponding coefficients. Here, f stands for the Laplace fundamental solution defined as $f(r) = \frac{1}{4\pi r}$ with $r = |x-y|$ is the euclidean distance between two points x and y.

When using Dirichlet and Neumann conditions we obtain the linear system $Ax = b$, with A being the transfer matrix and:

$$x = (a_0, a_1, \cdots, a_M)^T$$
$$b = (u_{x_1}, \cdots, u_{x_N}, 0, \cdots, 0)^T$$

To find the unknown coefficients ($\mathrm{a}_i \in \mathbb{R}^{\mathrm{M+1}}$) and compute the potential on the heart, we solve the following least-square optimization problem with a Tikhonov regularization,

$$\|Ax-b\|^2 + \lambda\|Lx\|^2, \qquad (1)$$

where L the regularization operator is an identity matrix for the zero-order Tikhonov and λ is the regularization parameter to be identified.

4. Data-analysis

In order to assess the error related to the geometry variability from the error related to the inverse problem method we designed two test cases, with and without model uncertainty. In the first test case (Test A), the BSP computed using the i^{th} shape model (BSP_i) is used for the ECGI estimation only for the i^{th} shape model. As the second test case (Test B), the BSP^* generated using a reference cardiac shape model was used for the ECGI estimation for all 262 shape models.

For both test A and B and for each stimulation protocol, we computed 262 inverse solutions. Per solution, we calculated the corresponding activation times and the estimated site of initial activation. Afterwards, we computed the correspondence between the reconstructed and true activation maps by means of Pearson's correlation coefficients (CCs). Finally, we computed the Euclidean distance between the true pacing sites and the ECGI based earliest activation sites (EAS) obtained from the inverse solutions we denote as the Localization Error (LE).

Results

In Figure 3, the mean cardiac shape model with average activation times obtained from the ECGI based solutions from 262 shape models. The columns correspond to the true activation maps (left column in Figure 3) as used to

compute BSP, the mean activation maps for test A (middle column) and test B (right column). The rows correspond to the four stimulation protocols.Visually, there are no significant difference between the true activation sequence and the ECGI estimation in case of LV, RV and apical pacing. In the case of septal paced beats, we observe from the representation of the average activation map that, for both tests A and B, zones of low activation times in the RV and LV cavities. This finding would eventually be evidenced in the lower coefficient correlations and source location accuracy.

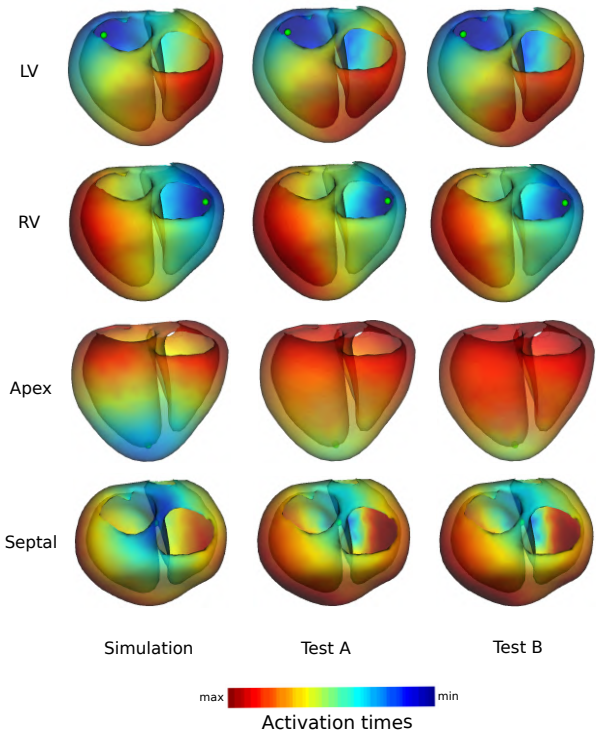

Figure 3. Comparison of activation times (from left to right): true activation times on the mean heart with green dots representing the average of the simulated excitation origin and reconstructed activation times on the average heart (test A & B) with red dots representing the average earliest activation sites calculated by MFS.

The box plots for spatial CCS of the activation maps for all models are provided in Figure 4. In the four stimulation protocols, we remark a small decrease of the CC values from 0.959 $\pm$ 0.006 (in Test A) to 0.950 $\pm$ 0.007 (in Test B) for LV paced beat, from 0.951 $\pm$ 0.014 to 0.943 $\pm$ 0.018 for RV paced beat,from 0.935 $\pm$ 0.014 to 0.911 $\pm$ 0.016 for apical paced beat and from 0.819 $\pm$ 0.045 to 0.797 $\pm$ 0.071 for septal paced beat.

From the obtained ATs we compute the earliest activation sites. These latter are projected on the average cardiac shape model and depicted in Figure 5. Qualitatively, the distribution of EAS based on the MFS is not different in tests A and B with a few exceptions which mainly concern the Endo/Epi localization of the EAS. The Euclidean distances between the true pacing sites and the ECGI based earliest activation sites (EAS) for the four stimulation protocols are reported in the box plots in Figure 6. If no model uncertainty (Test A), the errors (mean $\pm$ standard deviation) for LV, RV, apex and septal pacing are 11.3 $\pm$ 5.1, 7.0 $\pm$ 3.5, 14.6 $\pm$ 2.5 and 14.0 $\pm$ 5.5mm, respectively. Whereas under model uncertainty (Test B), the errors for LV, RV, apex and septal pacing are 11.6 $\pm$ 5.4, 5.0 $\pm$ 1.9, 12.2 $\pm$ 4.2 and 15.8 $\pm$ 5.5mm, respectively.

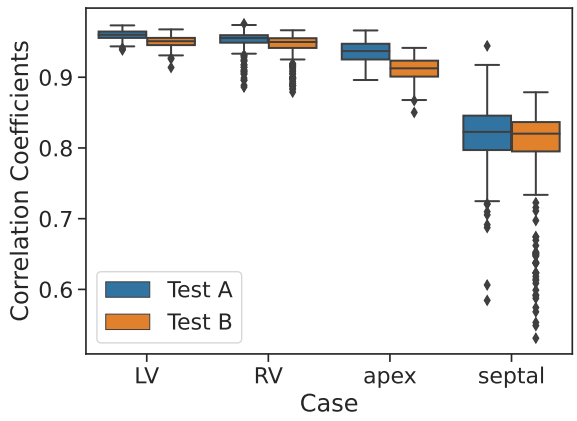

Figure 4. Correlation coefficients of the reconstructed activation maps in the four stimulations protocols.

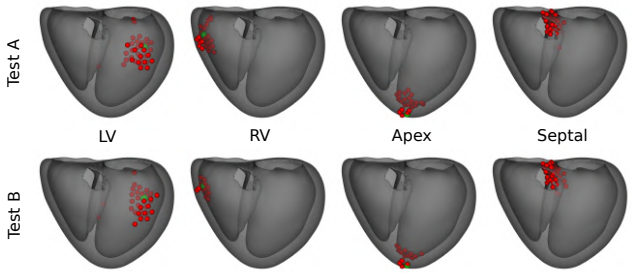

Figure 5. Pacing sites with green dots. MFS based earliest activation sites with red dots.

Discussion and Conclusion

With a focus on segmentation uncertainty, we used computed BSP with the same or a reference heart shape to estimate the activation sequence. In fact, we performed two tests A and B. In test A, we solved the inverse problem for each cardiac shape model given the corresponding BSP.

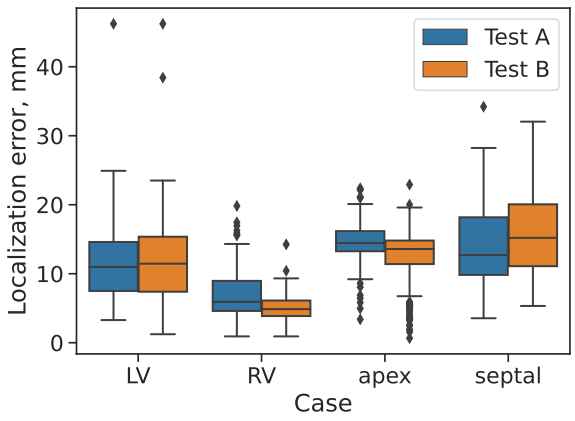

Figure 6. Box plots of the localization error of the pacing site using Euclidean distance.

In test B, we solved the inverse problem for the different shape models starting from one single BSP. Afterwards, we evaluated, for both tests A and B per stimulation protocol, the correlation coefficients between the reconstructed and true activation maps as well as the localization errors of the ectopic ventricular sites given the position of ECGI based excitation origins. The obtained results indicate that the segmentation uncertainty affected the resulting activation maps for all the stimulation sites but this was not observed on the source localization, particularly for the RV and Apex stimulation. This could be explained by the low variability across the 262 cardiac shape models of the chosen stimulation sites. In fact, an analysis of the computed BSPs for these cases shows the effect of the segmentation on the amplitude of the signals but rarely on the morphology which is more likely to affect the ECGI results.

As the results from Test A indicate, there remain additional sources of uncertainty which likely affects the ECGI estimations. During real-life BSP measurements, beat-to-beat differences occur due to respiration. The respiratory directly affects the position of the heart within the torso and consequently the obtained BSP. Furthermore, as patient-specific images are however obtained at one respiratory state during CT/MRI imaging procedures; either end-respiratory or end-excretory. To partially reduce this error mathematical models have been proposed [7]. Another part of uncertainty is expected for the repolarization due the contraction of the heart as we only use the end of diastolic phase from the imaging for the segmentation.

In future work, we will extend our study to different stimulation sites in areas of the heart more affected by segmentation variability. As it has shown that the largest variation was found at the base of the heart we may observe that also earliest site of activation may be significantly affected by cardiac shape model differences if we specifically assess stimulation protocols in these areas.

Acknowledgements

This Project has received funding from the European Unions Horizon research and innovation programme under the Marie Skodowska-Curie grant agreement No. 860974 and by the French National Research Agency, grant references ANR- 10-IAHU04-LIRYC and ANR-11-EQPX-0030. This project was supported by the National Institute of General Medical Sciences of the National Institutes of Health under grant numbers P41GM103545, R24GM136986, U24EB029012, U24EB029011, R01AR076120, and R01HL135568. Data used in this study was made available by Drs. John Sapp and Milan Horacek and their research collaboration with Dalhousie University. The authors would like to thank all who generously provided the segmentations used in this study.

References

[1] Tate JD, Zemzemi N, Good WW, van Dam P, Brooks DH, MacLeod RS. Effect of segmentation variation on ecg imaging. In 2018 Computing in Cardiology Conference (CinC), volume 45. IEEE, 2018; 1–4.

[2] Tate JD, Elhabian S, Zemzemi N, Good WW, van Dam P, Brooks DH, MacLeod RS. A cardiac shape model for segmentation uncertainty quantification. In 2021 Computing in Cardiology (CinC), volume 48. IEEE, 2021; 1–4.

[3] Tate JD, Good WW, Zemzemi N, Boonstra M, Dam Pv, Brooks DH, Narayan A, MacLeod RS. Uncertainty quantification of the effects of segmentation variability in ecgi. In International Conference on Functional Imaging and Modeling of the Heart. Springer, 2021; 515–522.

[4] Cates J, Elhabian S, Whitaker R. Shapeworks: particle-based shape correspondence and visualization software. In Statistical Shape and Deformation Analysis. Elsevier, 2017; 257–298.

[5] Sundnes J, Lines GT, Cai X, Nielsen BF, Mardal KA, Tveito A. Computing the electrical activity in the heart, volume 1. Springer Science & Business Media, 2007.

[6] Wang Y, Rudy Y. Application of the method of fundamental solutions to potential-based inverse electrocardiography. Annals of biomedical engineering 2006;34(8):1272–1288.

[7] Bergquist JA, Coll-Font J, Zenger B, Rupp LC, Good WW, Brooks DH, MacLeod RS. Reconstruction of cardiac position using body surface potentials. Computers in Biology and Medicine 2022;142:105174.

Address for correspondence:

Narimane Gassa
INRIA Bordeaux sud-ouest
200 Avenue de la Vieille Tour, 33405 Talence
narimane.gassa@inria.fr